Universidade do Minho
Escola de Ciências

TECHNICAL REPORT

Thermo-Mechanic Response of a Ceramic Material Coated with Gold

Joaquim Carneiro, Pedro Carvalho, Filipe Costa

Customer

C - T A C
Territory, Environment and Construction Research Centre
(Prof. Doutor Said Jalali)

February 2010

Table of Contents

1. Morphologic characterization 3

1.2. Compositional characterization 4

1.3. Structural characterization 5

2. Structural stability characterization 6

Conclusions 11

TECHNICAL REPORT

Thermo – Mechanic Response of a Ceramic Material Coated with Gold

The present report has as the main objective to obtain, via the experimental process, the thermal response of a ceramic material coated with gold, when subjected to a variation of temperature. Under this context, the main information that it is important to be obtained consists in the calculation of the specific deformation, ε of the composite material (ceramic substrate coated with a gold top layer) that it is generated due to a temperature variation of about 100ºC.

This information is of extreme importance because it imposes the adoption of specific techniques to be implemented in civil construction. It must be enhanced that the experimental activity also considered the study of the chemical composition and the morphology of the materials that were supplied by the manufacturer. In fact, this is essential information, since its knowledge helps to correlate and to interpret the thermo-mechanics response.

1. Morphologic characterization

Scanning Electron Microscopy (SEM) was performed in order to investigate the morphology of the material. From Fig. 1 it is possible to observe that the sample is basically composed of two different materials, one with morphology typical of a "*glass type*" compound and another corresponding to a ceramic material. The "*glass type*" compound present holes of diameters that vary from ~ 40 to ~150 microns, probably due to air trapped inside the material during the fabrication process. The ceramic material presents a dense morphology indicating high quality material.

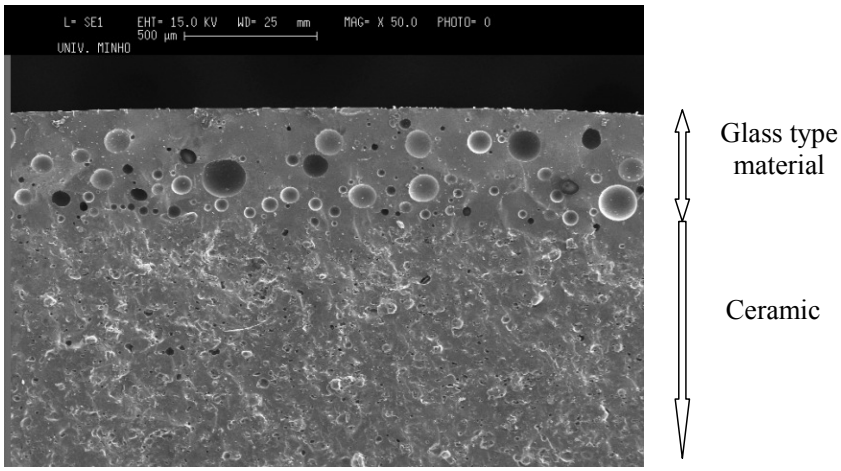

Fig. 1 - SEM image of the cross section of the analysed sample

Fig. 2 shows a detail image of the both regions, that is, the ceramic material and the "*glass type*" material. From this picture it is possible to observe a high dense ceramic material (Fig. 2a) and a high dense material ("*glass type*") with the already referred inside holes.

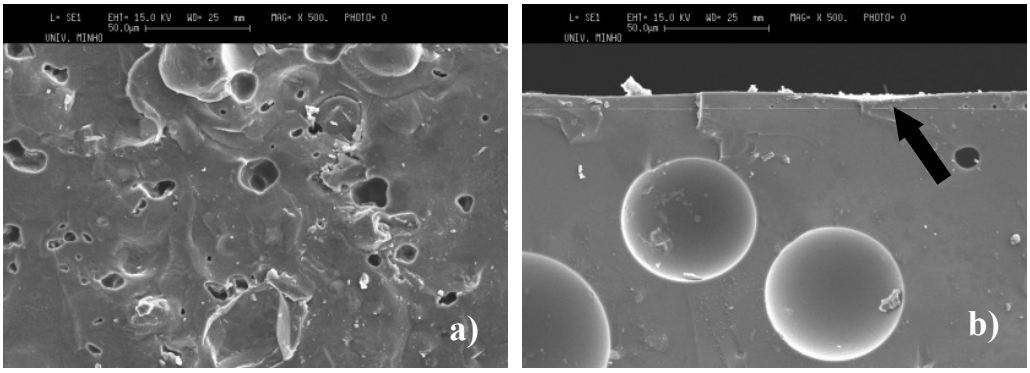

Fig. 2 - SEM image of the cross section of the a) ceramic material and b) "*glass type*" material

A close look into Fig (2b) it is possible to observe that this zone presents a top layer distinct from the "*glass type*" material. Fig. 3 presents the top layer in the "*glass type*" material. From this picture it is possible to observe that this top layer presents a similar density and morphology regarding the "*glass type*" material.

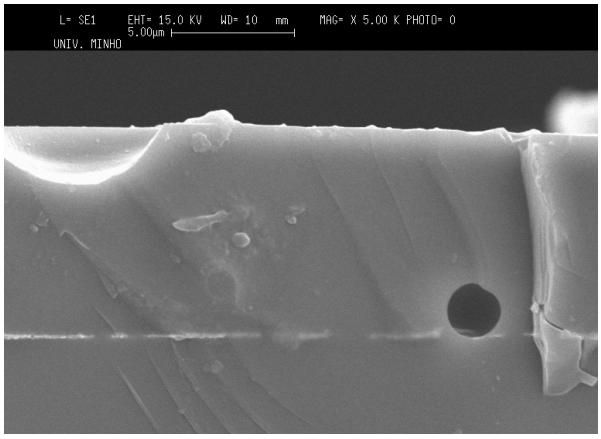

Fig. 3 - SEM image of the top layer in the "*glass type*" material

1.2. Compositional characterization

In order to understand this difference in the "*glass type*" material, an Energy Dispersive X-ray Analysis (EDX) was performed. Fig. 3 presents the EDX results from the top layer and the "*glass type*" material.

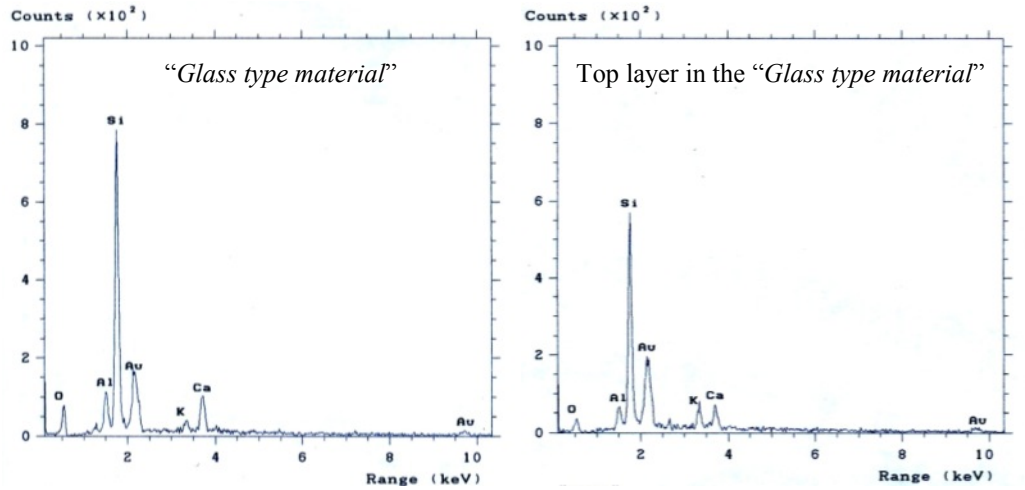

Fig. 3 - EDX spectra of the top layer and the "*glass type*" material

From the analyses of the relative peak intensities of the elements characteristics of a "*glass type*" material (Si, Al, O, K and Ca) and the gold (Au) peak (see Fig. 3) we can conclude that the top layer in the "*glass type*" material is gold rich regarding the "*glass type*" material. It must be referred that the gold (Au) peak of the "*glass type*" material should result from the deposited Au thin film before the SEM analyses.

From the SEM and EDX analyses one hypotheses start to grow: this material is composed by a ceramic substrate covered by a "*glass type*" material with a gold rich top layer. In order to further understand the nature of this top layer a XRD analyses was performed.

1.3. Structural characterization

Fig. 4 presents the XRD spectrum of the top layer in the "*glass type*" material.

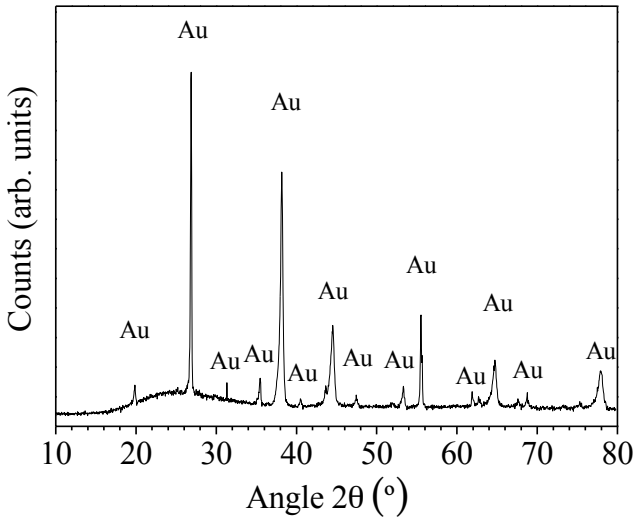

Fig. 4 - X-ray diffraction patterns of the top layer.

From X-ray diffraction analysis (Philips PW 1710 X-ray diffractometer) we can conclude that all the diffraction peaks correspond to gold (Au). Comparing the relative peaks intensity with the JPCDS data we can strongly suggests that Au is in a ***powder form***.

2. Structural stability characterization

For several years a range of optical profilometers and microtopographers were developed at the Physics Department of the University of Minho aiming different applications, the MICROTOP' family, improved and adapted according to particular inspection needs.

The former system, the MICROTOP.03.MFC, was based on a method involving optical active triangulation (Fig. 5) with oblique incidence and normal observation, and mechanical sample's scanning.

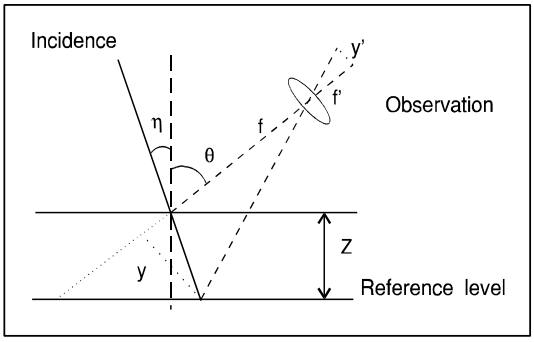

The relation between the measured value (y') and height (Z) comes:

$$y' = M \frac{Z \sin(\eta + \theta)}{\cos\eta + (Z/f)\cot(\eta + \theta)}$$

where $M = f / f'$ is the optical magnification in the observation arm, f and f' are the focal lengths of the observation optics, η the incidence angle and θ the observation one.

Fig.5 - A sketch of the general triangulation geometry

Now another triangulation arm is incorporated on the sensor's head allowing specular triangulation with resolutions down to the nanometer range. Furthermore when using a line-scan scan camera with 2048 elements, pitch 13μm the roughness of smoother samples can be measured by an angular resolved scattering approach. If on the specular observation arm a differential photodiode is employed a resolution of a few nanometer are achieved on the inspection of smooth surfaces. A CCD camera with a coaxial illuminator allows 2D images to be acquired and processed. In the MIROTOPO.06.MFC incorporating angle resolved scattering methods extended the method.

The experimental setup and the inspection process are represented in Fig. 6 and it is briefly described next.

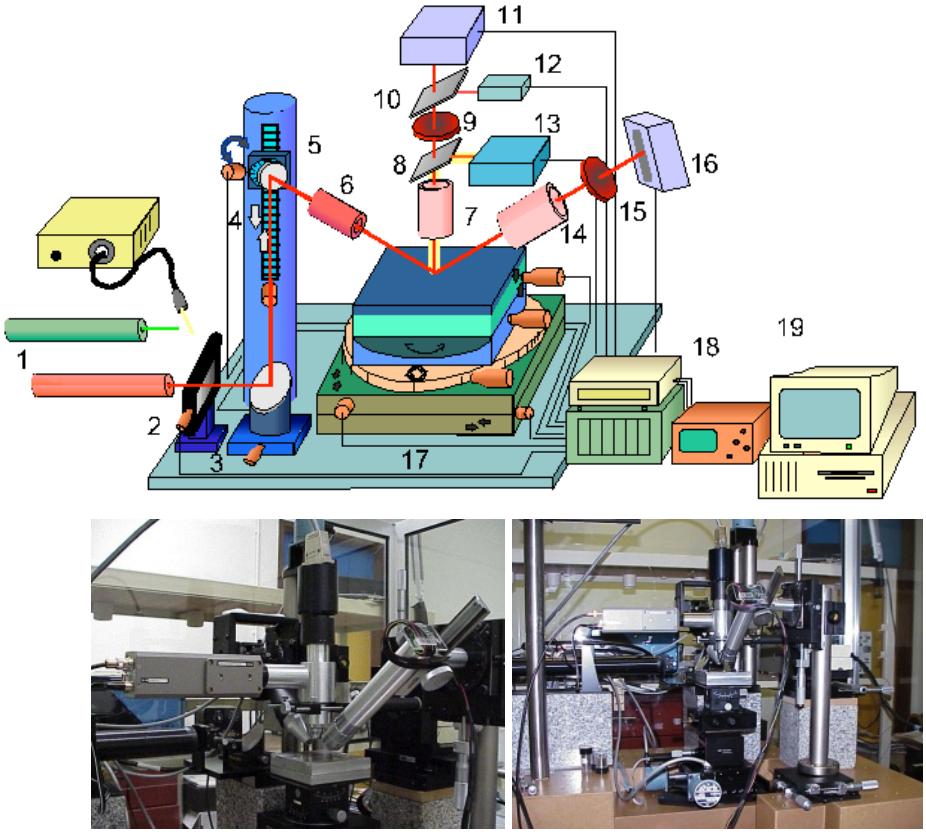

Fig. 6 – 1) Interchangeable light sources; 2) Vibration isolation stand; 3) Neutral density filter; 4) Beam steering system; 5) Incidence angle control motorised system; 6) Incidence optics; 7) Normal observation optics; 8) and 9) Beam splitters; 10) Interference filter; 11) Normal photosensitive detection system; 12) Photodetector; 13) Video camera and illuminator; 14) Specular observation optics; 15) Interference filter; 16) Specular photosensitive detection system 17) Sample support and motorised positioning system; 18) Data acquisition and control system; 19) Microcomputer

The incidence set-up comprises apart from the light source a neutral density variable filter, a motorised beam steering system, a spatial filter and focusing optics. The change on the incidence angle is made synchronised with the change of the observation angle on the specular arm. A vertical movement precision stage endowed of computer controlled motion provided by a reliable accurate DC encoder with high positioning repeatability and resolution is used refocusing of the observation optical system but especially for calibration of both arms of the sensor. In order to resolve shaded areas and mutual reflections, a high precision rotational stage is used allowing easy change to opposite light incidence. Often the faces of the surface to be analysed are not parallel or simply the surface to be inspected does not lie horizontally. In order to maintain the best height resolution a tilt table was incorporated to the samples' positioning system.

Furthermore it may allow the inspection of 3D objects or surfaces with pronounced holes of it, for instance (see Fig. 7).

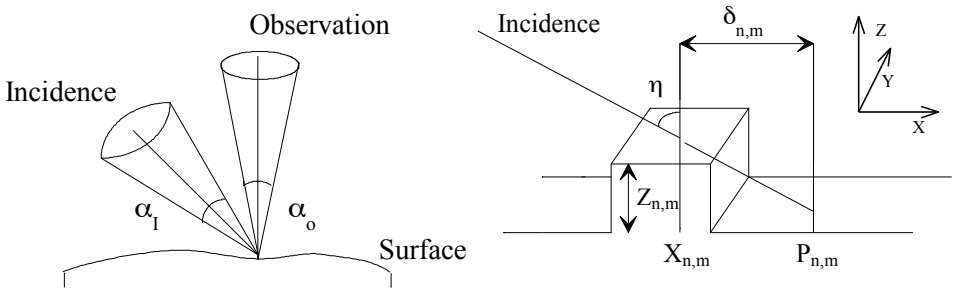

Fig. 7 – The surface's relief inspection system we implemented is based on the geometry sketched above. The intersection of an oblique light beam with an opaque surface creates on it a bright spot whose lateral position depends on the surface height.

In order to obtain the specific deformation, ε of the sample, the gold coated ceramic composite was heated up to 150ºC and after stabilization, it was cooled (natural cooling) to 50ºC.

The sample thickness was measured before and after heating and along the cooling down process. The longitudinal and transversal deformation was measured by measuring the change on the distance between the slope of two parallel scratch made with a diamond tip. Forty profiles where measured. Relief maps were also obtained and roughness characterization parameters calculated according to ISO standards (ISO 4287, ISO 12085 and ISO 1565-2).

All the measures where performed, in the 3 dimensions (see Fig.8), using the laser microtopographer MICROTOPO.06.MFC developed at the Microtopography Laboratory of the Physics Department. The system was set in a configuration with a resolution in lateral measures of 0.1microns and in height measures of 0.03microns.

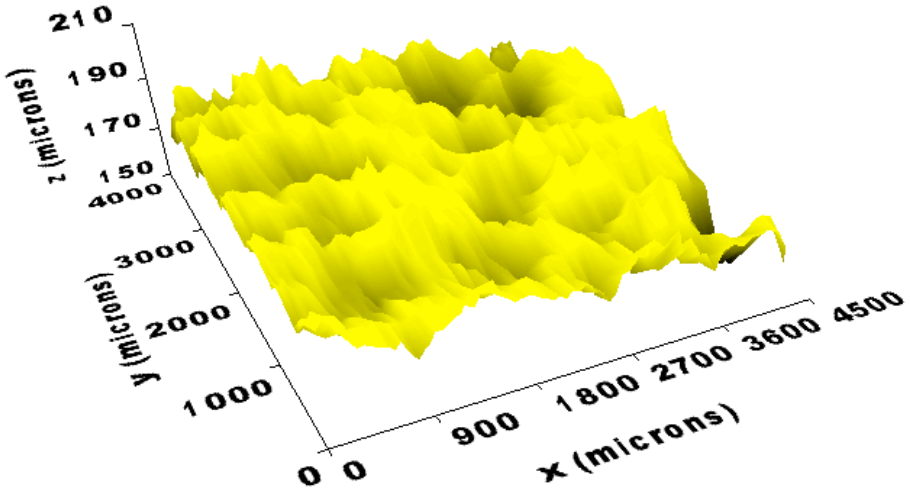

Fig. 8 – Texture of the gold coated ceramic surface

Fig. 9 is a 3D map of the gold coated ceramic surface obtained before and after heating, respectively.

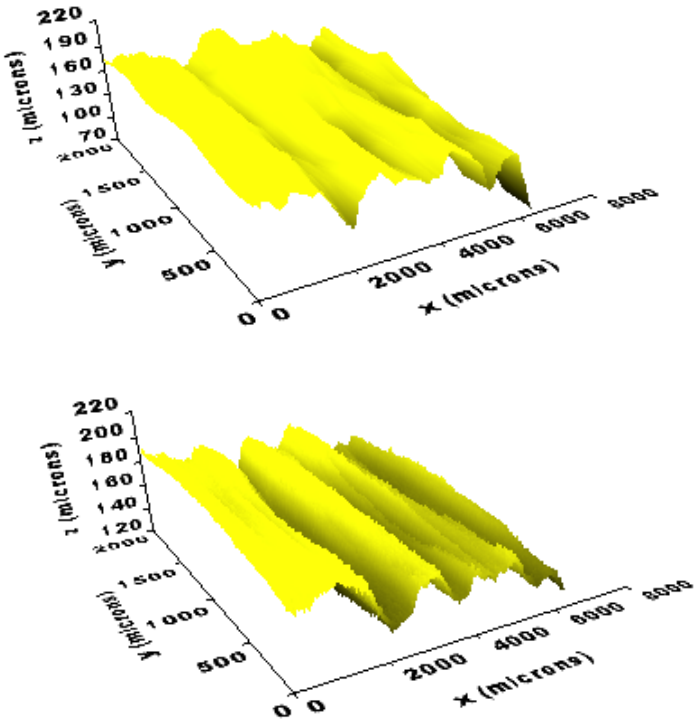

Fig. 9 – Relief maps obtained immediately before (above) and after heating up to 150ºC (below). The texture of the surface appears rougher and the scratches made on the surface before the measures also appear more defined.

The roughness parameters (map on Fig. 9) both average roughness (average of the surface height distribution), *Ra*, root mean square roughness *Rq* and total height *Rt* (measure of the height difference between highest peaks and deepest valleys) registered a roughly 10% increase.

In both samples the skewness (vertical symmetry factor) are low but even lower after heating. This means that the slight (minor) predominance of peak before the heating process is eliminated into a vertically symmetrical structure. The small reduction on average wavelength, *la*, and average peak spacing, *Sm*, results from the increase on roughness. The coincidence between the values obtained from profiles and the 3D parameters **illustrates the isotropy of the surface.**

Fig. 10 is the relief maps *obtained immediately after cooling down during 5 minutes*; a slight difference is noticed.

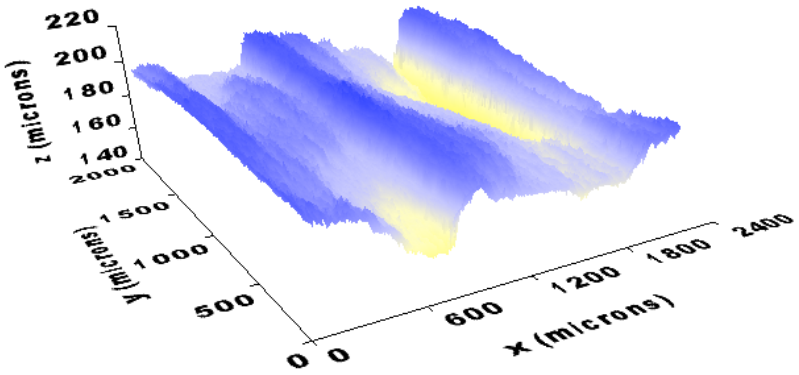

Fig. 10 – Relief map immediately after cooling down during 5 minutes

In the graph of Fig. 11 is shown a series of profiles (unfiltered: roughness profile P) obtained immediately after heating and at regular time intervals during the cooling process. The elastic reduction of lateral expansion and height shrinkage to ground level appears clearly. In the range of the employed heating temperatures the deformation is elastic in the three dimensions. The deformation seems to be isotropic in both transversal and longitudinal direction.

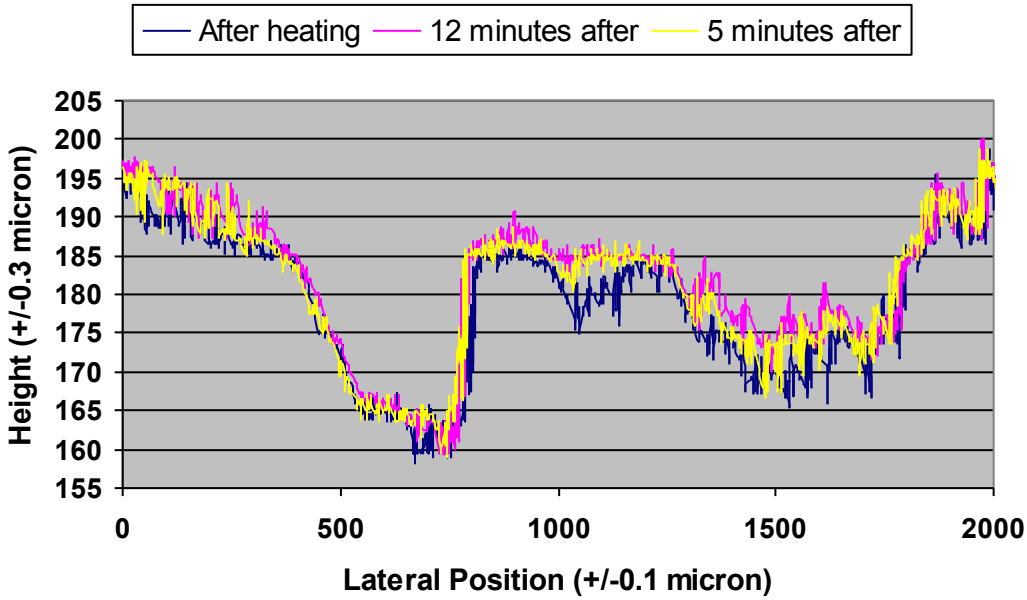

Fig. 11 – Series of roughness profiles obtained immediately after heating and at different time intervals during the cooling process

From the shift between the series of roughness profiles (see Fig. 11), it is possible to calculate the specific deformation, ε of the "*glass type*" material with a gold rich top layer. An average **lateral (longitudinal or transversal) expansion** of **29.8 +/-2.3** microns and a **height deformation** of **3.27+/-0.42** microns were measured.

Knowing that the initial (before heating) lateral length of the sample was L_0 = 1mm and the initial thickness was H_0 = 8mm and the temperature variation was ΔT = 100 ºC (150 – 50 =100 ºC) then:

– **Average lateral specific deformation**: $\varepsilon_L = \frac{\Delta L}{L_0} \approx \frac{30}{1000} = 0.03 = 3\%$

– **Average height specific deformation:** $\varepsilon_H = \frac{\Delta H}{H_0} \approx \frac{3.3}{8000} \approx 0.043\%$

– **Average lateral expansion coefficient:** $\alpha_L = \frac{\varepsilon_L}{\Delta T} \approx \frac{0.03}{100} = 3 \times 10^{-4} / {}^{\circ}C$

Conclusions

This sample is composed by high quality ceramic substrate covered by an amorphous "*glass type*" material with a gold rich top layer. This gold rich top layer should result from the introduction of gold particles in the amorphous matrix "*glass type*" material. The amorphous nature of this matrix combined with the high the presence of pores should play an important role in the mechanical properties of the sample.